1 Title

2 fCO_2^{sw} variability in the Bay of Biscay during ECO cruises

3

4 Authors

5 Padín, X.A. [1], Castro, C.G. [1], Ríos, A.F. [1] and Pérez F.F. [1]

6 [1] Instituto de Investigaciones Marinas, CSIC, Eduardo Cabello, 6, 36208 Vigo, Spain

7

8 Corresponding e-mail address

9 padin@iim.csic.es

10

11 Abstract

12 The Bay of Biscay is part of the North Atlantic Ocean, the most important sink of CO_2,

13 and a subduction zone of mode waters that favours the entry of carbon to the ocean

14 interior. To investigate the seasonal and interannual variability of CO_2 uptake,

15 continuous underway measurements of the partial pressure of CO_2 at sea surface were

16 performed along a commercial route between Vigo (Spain) and St. Nazaire (France).

17 An unattended measuring system of CO_2 fugacity (fCO_2), with meteorological station,

18 and temperature, salinity, oxygen and fluorescence sensors, was installed on board of

19 ships of opportunity (*RO-RO L'Audace* and *RO-RO Surprise*).

20

21 The dataset collected between December 2002 and December 2004 reported a

22 significant interannual variability; mainly for the winter season. The noticeable increase

23 of fCO_2^{sw} during the winter mixing period of 2004 was associated to biogeochemical

24 differences related to nutrient ratios, phytoplankton activity and atmospheric CO_2

25 uptake. Dividing the seasonal cycle into three periods, prebloom (October – February),

bloom (March – May) and postbloom (June – September), the fCO_2^{sw} for the entire seasonal cycle was correctly predicted by empirical relationships with an error lower than 10 µatm in spite of the high interannual variability. The fCO_2^{sw} variability at seasonal scale was mainly controlled by processes of synthesis and remineralization of organic matter during prebloom and bloom periods whereas SST was the key parameter during postbloom period. The surface waters of the Bay of Biscay showed a clear role as atmospheric CO_2 sink ranging from -2.7±2.8 (±0.3) to -0.08±0.41 (±0.04) molC·m^{-2}·yr^{-1} (*mean±standard deviation (±error)*) throughout each complete period although CO_2 release to atmosphere was also observed during short episodes of summer. Using the regular wind speed sources of CO_2 fluxes estimation ranged from -1.3±1.7 (±0.1) to -2.4±2.7 (±0.1) molC·m^{-2}·yr^{-1} at annual scale, exceeding the sink capacity of the nearby regions of the North Atlantic Ocean.

INTRODUCTION

The world's oceans are currently a net sink for atmospheric CO_2 uptaking to almost half of all fossil-fuel emissions (Sabine et al., 2004). The capacity of the oceans to absorb the CO_2 excess plays a relevant role in the global warming mitigating the effect of greenhouse gas emissions. Therefore quantification of oceanic CO_2 uptake is a key for understanding the interactions and feedbacks between the carbon system and the overall earth system. These interactions were the aim of multiple research programs in the past decade (e.g. Tans et al., 1990; Sarmiento et al., 1995; Wallace, 1995; Gruber et al., 1996; Brewer et al., 1997; Takahashi et al., 1997) but the exact magnitude of the variability has not been completely constrained (Gruber et al., 2002; Watson et al., 1991). The disagreements between ocean models (Le Quere et al., 2000) and atmospheric inversions (Peylin et al., 2005) in relation to interannual variability of the CO_2 global sink also emphasize the poorly constrained variability.

The knowledge of the ocean carbon cycle would improve by extending the CO_2 observations to larger areas for several years. Global carbon models (Sarmiento et al., 1992; Maier-Reimer and Hasselmann, 1987) need appropriate dataset for model testing or to assimilating in the new update models. To accomplish this objective, autonomous CO_2 probes are increasing the frequency and spatial coverage of measurements. Besides research vessels, ships of opportunity (Lüger et al., 2004; Padin et al., 2007 a,b), time series-stations (Gruber et al., 2002; Dore et al., 2003; Gonzalez-Davila et al., 2003) and drifter buoys (Copin-Montégut and Avril, 1993; Lévy et al., 1998; Andersen and Prieur, 2000; Hood and Merlivat, 2000) are becoming suitable platforms to develop ambitious sampling strategies. Empirical algorithms are also used to extrapolate CO_2

76   partial pressure (pCO_2) observations in relation to even retrieved parameters from

77   remote sensing (Tans et al., 1990; Metzl et al., 1995; Stephens et al., 1995; Goyet et al.,

78   1998; Lee et al., 1998; Hood et al., 1999; Nelson et al., 2001; Lefevre and Taylor, 2002;

79   Olsen et al., 2004).

80

81   A large part of these measurements has been carried out in the North Atlantic Ocean

82   due to its outstanding role as CO_2 sink among oceanic regions (Takahashi et al., 2002).

83   The formation of mode waters due to seasonally deep mixing and the notable

84   phytoplankton activity yield the intense CO_2 absorption of the North Atlantic.

85   Following these research efforts, our project (ECO: Evolution of CO_2 increase using

86   ships of opportunity: Galician coast and Bay of Biscay) was developed with the aim of

87   intensifying the CO_2 recordings in the Bay of Biscay. This regional sea has an

88   important role in the subduction of mode waters in the North Atlantic Ocean (Paillet

89   and Mercier, 1997) and represents one of the areas with the highest accumulation of

90   anthropogenic CO_2 (Gruber, 1998).

91

92   In order to improve the description of the carbon cycle in the Bay of Biscay, an

93   unattended measuring system of CO_2 fugacity (fCO_2) was installed on board of ships of

94   opportunity. Additionally key physical and biological parameters were monitored to

95   evaluate their relevance in the CO_2 variability at seasonal and interannual scale.

96   Underway measurements were performed along 150 tracks from November 2002 to

97   December 2004. The purpose of this work is to constrain the assessment of CO_2 flux as

98   well as to describe the role of different drivers of fCO_2 distribution during ECO cruises.

99

100   MATERIALS AND METHODS

101

The dataset presented in this paper was collected on board of ships of opportunity from Flota Suardíaz Company (*RO-RO L'Audace* and *RO-RO Surprise*) between December 2002 and December 2004. he regular route linked Vigo (Spain) and St. Nazaire (France) with a frequency of 12 transects per month, measuring more than 150 tracks throughout two entire seasonal cycles.

107

Seawater was continuously pumped from 3 meters below waterline into the ship's hull. The volume of water was pumped at a high flow rate although a smaller flow was only shunted through the analytical system in order to reduce the warming of the water on the way. Afterwards the uncontaminated seawater supply was bifurcated to pass through an analytical system composed by thermosalinometer (SBE-45-MicroTSG), oximeter (SBE-43) and fluorometer (WETLabs) and through a home made fCO_2 analyser. The underway measurements of sea surface salinity (SSS), sea surface temperature (SST), oxygen (O_2) and chlorophyll *a* concentration (chl a) were recorded with CO_2 fugacity in seawater (fCO_2^{sw}) and atmosphere (fCO_2^{atm}).

117

The measurements of CO_2 mole fraction (xCO_2) were performed with a non-dispersive infrared gas analyser (LI-6262). This analyzer was calibrated at the beginning and end of each transit using two gases; one of CO_2-free air and one of high CO_2 standard gases with a certified concentration of ~375 ppm (Instituto Meteorológico Nacional, Izaña, Canary Islands).

123

xCO_2^{sw} was converted into fCO_2^{sw} in saturated water vapour pressure using the atmospheric pressure measured with the analysis unit as described in DOE Handbook

126 (1994). Subsequently fCO_2^{sw} values were corrected for the temperature shift by means

127 of an empirical equation (DOE, 1994), originally proposed by Takahashi et al. (1993).

128 The temperature difference between the seawater inlet and the equilibrator system was

129 typically less than 1ºC.

130

131 During the ECO cruises atmospheric xCO_2 (xCO_2^{atm}) was measured every hour,

132 recording twenty observations within 5 minutes. Subsequently, a selection criteria was

133 applied to eliminate spurious values and to identify xCO_2^{atm} representative data. These

134 data were fitted to a seasonal curve, consisting of an annual trend plus a seasonal cycle

135 (Padin et al., 2007b). To convert xCO_2^{atm} into pCO_2^{atm} (Equation 1) water vapour

136 pressure (pH_2O, in atm) was calculated from *in situ* temperature (Tis, in ºC) according

137 to Cooper et al. (1998) (Equation 2). Following Olsen et al. (2003), a decrease of 0.3%

138 from pCO_2^{atm} to fCO_2^{atm} (Weiss, 1974) was considered accurate enough.

139

140
$$pCO_2^{atm} = xCO_2^{atm} \cdot (patm - pH_2O) \qquad\qquad (1)$$

141
$$pH_2O = 0.981 \cdot \exp(14.32602 - (5306.83/(273.15 + Tis))) \qquad (2)$$

142

143 Discrete samples were collected at four locations along the commercial track (46±0.3ºN

144 -4.7±0.5ºW; 45.5±0.2ºN -5.6±0.3ºW; 45±0.2ºN -6.7±0.3ºW; 44.5±0.2ºN -7.7±0.3ºW)

145 (*mean±standard deviation*) to calibrate the different sensors (Fig. 1). The calibration

146 frequency changed during the ECO project from three per month during 2003 to one

147 per month during 2004.

148

149 Alkalinity (A_T) and pH and measurements were done to study the internal consistence

150 of *in situ* fCO_2^{sw} measurements. Poisoned A_T samples, as the DOE handbook (DOE,

151 1994) recommends, were determined by automatic potentiometric titration with HCl at

152 a final pH of 4.40 (Pérez and Fraga, 1987). The electrodes were standardised using a

153 buffer of pH 4.42 made in CO_2 free seawater (Pérez et al., 2002). The method has an

154 accuracy of ±1 µmol/kg estimated using Certified Reference Material (CRM). The pH

155 samples were kept refrigerated since collection until the spectrophotometric

156 determination following Clayton and Byrne (1993). This method has a precision of

157 0.00004 and an accuracy (Clayton and Byrne, 1993) of 0.002 (DelValls and Dickson,

158 1998). The comparison between the *in situ* and the computed fCO_2^{sw} from pH and A_T

159 using the carbonic system constants of Lueker et al. (2000), showed a consistence error

160 of ±6 µatm (n = 365, r^2 = 0.91).

161

162 Discrete oxygen samples were stored in the dark and analyzed by the Winkler method

163 24 hours after collection. The potentiometric end-point determination of oxygen has an

164 estimated accuracy of ±2 µmol·kg^{-1}. Oxygen saturation was calculated following

165 Benson and Krause equation (UNESCO, 1986). The underway fluorescence

166 measurements, determined with a WETLabs fluorometer, were calibrated with

167 chlorophyll extracted by 25mm Whatman GF/F filters and analyzed after 90% acetone

168 extraction in a 10,000 R Turner fluorometer (Yentsch and Menzel, 1963). The precision

169 was ±0.05 mg·m^{-3}.

170

171 Additionally, the nutrient samples were also collected in polystyrene bottles and stored

172 in the freezer at -30ºC prior to lab analysis. The concentration of nitrate (NO_3),

173 phosphate (PO_4) and silicate ($Si(OH)_4$) were determined by segmented flow analysis

174 with Alpkem autoanalyzers, following Hansen and Grasshoff (1983) with some

175　improvements (Mouriño and Fraga, 1985). The analytical errors are ± 0.05 $\mu mol \cdot kg^{-1}$

176　for NO_3, ± 0.05 $\mu mol \cdot kg^{-1}$ for $Si(OH)_4$ and ± 0.01 $\mu mol \cdot kg^{-1}$ for PO_4.

177

178　Air-sea CO_2 exchange

179　The exchange of carbon between the atmosphere and the ocean (F) was calculated with

180　the following equation:

181

182　$$F = k\ S\ (fCO_2^{sw} - fCO_2^{atm}) \tag{3}$$

183

184　Seawater CO_2 solubility (S, $mol \cdot L^{-1} \cdot atm^{-1}$) was calculated from Weiss (1974) and the

185　piston velocity (k, $cm \cdot h^{-1}$) was computed from coefficients reported by Nightingale et

186　al. (2000). In spite of the several formulations of piston velocity, the Nightingale's

187　parameterization was pointed out as the more consistent in recent findings (Ho et al.,

188　2006; Sweeney et al., 2007). The wind speed used in our computations was remotely

189　measured by QuikSCAT satellite with temporal and spatial resolutions of 0.25º and 12

190　hours, respectively. This dataset was collected from the Physical Oceanography Active

191　Archive Center of the Jet Propulsion Laboratory (http://podaac.jpl.nasa.gov).

192　Additionally daily mean (average of four measurements per day) of wind vector

193　product was also provided by the NCEP/NCAR reanalysis project (Kalnay et al., 1996)

194　from the web site of the NOAA-CIRES Climate Diagnostics Center, Boulder, Co, USA

195　(http://www.cdc.noaa.gov/). The wind speed from both sources was linearly

196　interpolated at temporal and spatial scale.

197

198　Winter mixed layer

199 Winter mixed layer (WML) depths were provided by the MERCATOR-OCEAN model

200 (http://www.mercator-ocean.fr) averaging a region of the Bay of Biscay between 44º to

201 46ºN and between 9º to 4ºW. The WML depth is estimated according to the density

202 criterion establishing the WML lower limit when the density difference is 0.05 kg·m^{-3}

203 from the surface value. This criterion was preferred to the temperature one, following

204 Kara et al., 2000.

205

206 RESULTS

207

208 Biogeochemical variability

209 The temporal evolution of the sea surface properties in the Bay of Biscay during the

210 ECO project showed a marked seasonality with two clear seasons, winter and summer

211 (Borja et al., 2000a). The SST pattern (Fig. 2) showed differences between 2003 and

212 2004 years, with seasonal ranges of 9.1 ºC and 9.5 ºC, respectively. The highest SST

213 values were reached during September 2003 (21.5ºC) and August 2004 (21 ºC) whereas

214 the coldest surface waters were found in February 2003 (12.4ºC) and January 2004

215 (11.5ºC).

216

217 Even though SSS distribution was nearly uniform for the two years (35.617±0.024

218 (±0.001) psu; Fig. 2), the precipitation–evaporation balance and the meteorological

219 conditions yielded an obvious seasonal pattern. During winter, the surface waters of the

220 Bay of Biscay get usually saltier due to the advection of southern saline waters

221 conveyed northward by the Iberian Poleward Current (Haynes and Barton, 1991).

222 Besides the winter mixing with subsurface saltier waters also contributes to the higher

223 winter SSS. The intensity of both contributions during the ECO cruises showed

224 appreciable differences since the resulting SSS increment was more sustained during

225 winter 2004. Contrary the lowest SSS values were measured during spring achieving

226 absolute SSS minimum, namely, 35.56±0.01 psu, during May 2003. These low SSS

227 values coincided with the thaw period reflecting the influence of runoff from Loire and

228 Garonne rivers that flow with a mean volume of ~2000 $m^3 \cdot s^{-1}$. The intense evaporation

229 during summer and the later stratification breakdown previous to the formation of

230 WML yielded the highest SSS of 35.651±0.021 (±0.004) psu in October 2003.

231

232 The winter convection yielded similar WML maxima during the successive years

233 reaching ~200 m (Fig. 3) at the middle of February and March, respectively. However

234 winter convection during 2004 lasted for almost one more month than in winter 2003.

235 The interannual variations in surface nutrient concentrations are associated with the

236 different vertical mixing pattern. The nutrient maxima (NO_3, PO_4 and $Si(OH)_4$) were

237 2.00, 0.27 and 2.00 $\mu mol \cdot kg^{-1}$ during winter 2003 and 5.51, 0.34 and 2.20 $\mu mol \cdot kg^{-1}$

238 during winter 2004. Besides the quantitative differences, the nutrient ratios were also

239 different for the two winter. The $NO_3:Si(OH)_4$ ratio for 2003 was 1.6 (±0.2) whereas

240 during 2004 it was 3.2 (±0.2) (Table 1). The $NO_3:PO_4$ ratios also showed interannual

241 variation during the successive winter mixing events reporting 14 (±3) and 18 (±1),

242 respectively. After reaching the maximum winter mixing (February 2003 and April

243 2004), the rapid shoaling of the mixed layer (Lochte et al., 1993) triggered the onset of

244 biological activity leading to complete NO_3 depletion (Fig. 2). On the other hand, the

245 phytoplankton consumption did not cause a total depletion of sea surface PO_4 and

246 $Si(OH)_4$ levels (Fig. 2).

247

248 A similar temporal evolution was observed for PO_4 and $Si(OH)_4$ concentrations

249 throughout the sampling periods. Both nutrients were gradually reduced during year

250 2003 reaching minimum values in September. The synthesis – remineralisation balance

251 of organic matter during year 2004 showed different distribution at seasonal scale

252 reporting an intense consumption during the bloom period. The spring bloom – just at

253 the total NO_3 depletion - was extended for a few weeks from the mid February to

254 middle April. The nutrient concentrations during the bloom period kept similar ratios to

255 the prebloom ones, namely, 1.8 (±0.5) and 4.1 (±0.5) for $NO_3:Si(OH)_4$ and 13 (±2) and

256 20 (±2) for $NO_3:PO_4$ during 2003 and 2004, respectively (Table 1).

257

258 The chl a distribution reached maximum values of 2.6 and 1.2 mg·m^{-3} coinciding the

259 more intense nutrient consumption during March 2003 and April 2004, respectively.

260 Contrary the surface chl a concentration decreased to minimum values due to the

261 nutrient exhaustion during the summer. The breakdown of the summer stratification

262 provoked the upwards input of nutrients to the sea surface reactivating the

263 phytoplankton activity in September.

264

265 The oxygen saturation varied from a minimum at the end of the summer period to a

266 maximum just after the bloom periods. The highest saturation values, oversaturation of

267 ~20%, were reached in June 2003 and July 2004 (Fig. 2).

268

269 Continuously recordings of $fCO_2{}^{sw}$

270 The seasonal evolution of $fCO_2{}^{sw}$ (Fig. 2) showed an identical variability with a range

271 of 72 µatm for the two seasonal cycles. Briefly, several features are shared by both

272 annual $fCO_2{}^{sw}$ cycles. During winter the Bay of Biscay displayed undersaturated

273   fCO_2^{sw} level in relation to atmosphere with an homogeneous value of approximately

274   340 µatm for both winters. After that, minimum fCO_2^{sw} values were registered in spring

275   probably caused by an intense phytoplankton growth. Subsequently, the summer SST

276   increase led the fCO_2^{sw} distribution to the highest values of the seasonal cycle. Finally,

277   during the autumn season fCO_2^{sw} diminished associated to the SST decrease.

278

279   However several events also showed notable differences between both seasonal cycles.

280   Thus the fCO_2^{sw} distribution during winter 2004 increased noticeably until reaching an

281   annual maximum in January 2004 (Fig. 2). This fCO_2^{sw} trend closely followed the

282   evolution of nutrient levels and WML depth even reproducing a rise across two pulses

283   between March and April 2004 (Fig. 2). The biological drawdown also yielded

284   differences in fCO_2^{sw} reaching different undersaturation levels (73 and 85 µatm for

285   2003 and 2004, respectively). For the two seasonal cycles, the recorded spring bloom

286   presented two periods regarding the relationship between fCO_2^{sw} and chl a; one

287   corresponding to peak (February – March) and another to senescent stages (April –

288   May) of phytoplankton growth.

289

290   The fCO_2^{sw} – chl a relationships during the intense CO_2 drawdown reached values of 42

291   (±6) and 60 (±2) µatm·m^3·mg^{-1} during 2003 and 2004 respectively, substantially

292   exceeded the valued registered (~17 µatm·m^3·mg^{-1}) by Watson et al. (1991) for the

293   spring bloom in the North Atlantic during the NABE cruises. On the other hand, the

294   photosynthetic activity for the subsequent senescent phase (Table 1) agreed with

295   reported parameters (Watson et al., 1991; Frankignoulle et al., 1996). The

296   thermodynamic control steered the Bay of Biscay surface waters to oversaturated levels

297 of 371 µatm during summer 2003. However the fCO_2^{sw} increase for summer 2004 was

298 not so intense, not exceeding fCO_2^{atm} levels (Fig. 2).

299

300 The influence of the biological processes and the temperature variability on the fCO_2^{sw}

301 distribution during the ECO cruises was evaluated estimating the variables $^BfCO_2^{sw}$ and

302 $^TfCO_2^{sw}$, respectively, according to Takahashi et al. (2002):

303

$$^BfCO_2^{sw} = fCO_2^{sw} \exp [0.0423 (SST_{mean} - SST)]$$

304

$$^TfCO_2^{sw} = fCO_2^{sw}_{mean} \exp [0.0423 (SST - SST_{mean})]$$

305

306

307 where $^BfCO_2^{sw}$ denotes the fCO_2^{sw} normalized to the annual mean SST (SST_{mean}) and

308 $^TfCO_2^{sw}$ represents the effect of SST distribution on the annual mean of fCO_2^{sw}

309 ($fCO_2^{sw}_{mean}$).

310

311 In other words, $^BfCO_2^{sw}$ is the fCO_2^{sw} distribution without the SST control, representing

312 the biological signal as well as other processes such as air-sea exchange and alkalinity

313 variations. The maximum $^BfCO_2^{sw}$ values are observed just at the end of the prebloom

314 periods nearly exceeding 403 and 437 µatm in both years. Subsequently the $^BfCO_2^{sw}$ is

315 drastically reduced, within a short period of time, due to the onset of phytoplankton

316 CO_2 uptake. Throughout the following months the net biological control reduces the

317 $^BfCO_2^{sw}$ in a similar way reaching the annual minima in midsummer, 275 and 279 µatm

318 for 2003 and 2004 respectively. After that heterotrophic processes raise $^BfCO_2^{sw}$ to the

319 winter values, establishing seasonal ranges of ~129 and ~159 µatm for 2003 and 2004

320 respectively. Hence, the range of $^BfCO_2^{sw}$ for the Bay of Biscay varies between

321 characteristic values of oligotrophic areas (~80 µatm) and typical values of productive

322   regions (~280 µatm). For the ECO cruises, 78% of the $^{B}fCO_2^{sw}$ variability was

323   explained by the NO_3 distribution ($^{B}fCO_2^{sw} = 313(\pm4) + 55(\pm7)\cdot NO_3 - 7(\pm2)\cdot NO_3^2$;

324   n=48) showing the strong link between the $^{B}fCO_2^{sw}$ variability and the photosynthesis –

325   respiration processes.

326

327   On the other hand, $^{T}fCO_2^{sw}$ distribution, meaning the SST control on fCO_2^{sw}

328   distribution, yielded similar ranges, namely, 145 and 141 µatm with SST amplitude for

329   9.1 and 9.5ºC for 2003 and 2004.

330

331   The monthly average variation of temperature control ($^{T}fCO_2^{sw}$) and biological control

332   ($^{B}fCO_2^{sw}$) are shown in Figure 4b. The combined effect of both controls yields the net

333   fCO_2^{sw} variability (white circles, Fig. 4b). The $^{B}fCO_2^{sw}$ variation reached maximum

334   phytoplankton absorption of ~-46 and ~-73 µatm at the bloom periods of 2003 and

335   2004 respectively. The biological CO_2 uptake continued throughout the postbloom

336   periods, being clearly evident in autumn 2003 with a reduction of ~35 µatm. The sign

337   of this biological control was inverted from November to February pointing to a

338   dominance of surface heterotrophic processes or CO_2 enrichment due to entrainment of

339   subsurface waters, mainly, during the prebloom 2004. Regarding the variability of the

340   temperature control, the minimum $^{T}fCO_2^{sw}$ was observed during autumn concomitant to

341   the water cooling developed in November 2003. Conversely, during warming periods

342   $^{T}fCO_2^{sw}$ showed higher values steered by SST increase. Maximum values of 58 µatm

343   were reached during both Junes.

344

345   The relative magnitude of biological and thermodynamic control was estimated as the

346   ratio of seasonal amplitude of $^{B}fCO_2^{sw}$ and $^{T}fCO_2^{sw}$. The temperature effect played a

347 similar role for the two years whereas the influence of the processes represented by

348 $^{B}fCO_2^{sw}$ showed an important interannual variability. Thus the fCO_2^{sw} variability

349 associated to the biological control for 2004 was 10% stronger than the thermodynamic

350 component of fCO_2^{sw} variability.

351

352 The analysis of the biogeochemical control on fCO_2^{sw} variability was extended

353 performing multiple linear regressions taking into account all the measured variables.

354 The variability of NO_3, PO_4, chl a, SSS and SST are good proxies of the different

355 processes that control the fCO_2^{sw} variability such as thermodynamic effect,

356 remineralization processes and organic matter synthesis. So, the role and percentage of

357 explained fCO_2^{sw} variability by each variable was assessed for the three periods of the

358 seasonal cycle, prebloom (October – February), bloom (March – May) and postbloom

359 (June – September). From here, the relationships considering only the significant

360 variables were established (Table 2).

361

362 During the prebloom period, the fCO_2^{sw} distribution was poorly explained (~40%) with

363 a small error of ±6.8 µatm that was associated to its homogeneous distribution from

364 October to February. Water mixing and photosynthetic activity depicted by NO_3 and

365 chl a, respectively, seemed to control the fCO_2^{sw} variation explaining 15% and 21% of

366 fCO_2^{sw} variability, respectively (Table 2). During the bloom period the synthesis of

367 organic matter, represented by PO_4, explained 77% of the total fCO_2^{sw} variability

368 yielding a predicted fCO_2^{sw} error of 10 µatm. In spite of playing a weak role for the

369 other periods, SST was the main factor controlling fCO_2^{sw} trend during the postbloom

370 period explaining ~65% of the total variability. Including every significant variables,

371   the explained variability of fCO_2^{sw} reached 80%, pointing out the prevalence of

372   physical processes during postbloom period.

373

374   Air-sea CO_2 exchange

375   The measurements of fCO_2^{sw} and fCO_2^{atm} (Fig. 2) in the Bay of Biscay indicated a

376   regular absorption of atmospheric CO_2 during the ECO cruises. The fCO_2

377   disequilibrium between seawater and atmosphere was -29±25 (±1) µatm and -36±20

378   (±1) µatm for 2003 and 2004 respectively. The maximum undersaturation of surface

379   waters in relation to the atmosphere was recorded during April 2004, reaching a fCO_2

380   gradient of ~-83 µatm. In contrast, the direction of CO_2 exchange was inverted during

381   August 2003 with an oversaturation of ~9 µatm with respect to the atmosphere.

382

383   The air-sea CO_2 fluxes were computed according to Equation 3, using wind speeds

384   retrieved from remote QuikSCAT sensor and Nightingale's coefficients. The amplitude

385   of daily CO_2 flux ranged from 1.2 to -20 molC·m^{-2}·yr^{-1} (not shown) and the average

386   flux was -1.52±1.89 (±0.08) molC·m^{-2}·yr^{-1} for the ECO cruises (Fig. 5). The net CO_2

387   uptake showed small interannual variability of -1.29±1.68 (±0.09) and -1.7±2.0 (±0.1)

388   molC·m^{-2}·yr^{-1} for 2003 and 2004 respectively. The behaviour of the Bay of Biscay as an

389   atmospheric CO_2 sink was evident throughout every considered partition of the

390   seasonal cycle. The average CO_2 flux was stimulated during both prebloom periods

391   to kinetic effect of intense winds (Fig. 5), reporting -1.9±1.7 (±0.1) molC·m^{-2}·yr^{-1}. The

392   CO_2 uptake for the two bloom periods was only -2.4±2.4 (±0.2) molC·m^{-2}·yr^{-1} in spite

393   of showing the maximum disequilibrium and the absolute maximum of weekly

394   absorption ~-8 molC·m^{-2}·yr^{-1} during the bloom 2004. The small fCO_2 gradient and the

395   weak wind speed during the successive postbloom periods yielded mean CO_2

396 exchanges of -0.08±0.41 (±0.04) and -0.58±0.59 (±0.05) $molC \cdot m^{-2} \cdot yr^{-1}$ for 2003 and

397 2004 respectively.

398

399 Wind speed is one of the main sources of uncertainty in the estimations of CO_2

400 exchange. Therefore the CO_2 fluxes were also estimated using wind speed values from

401 NCEP/NCAR model (Olsen et al., 2003). The known lower celerity of NCEP/NCAR

402 winds (Olsen et al., 2005, Padin et al., 2007b) compared to QuikSCAT values yielded a

403 26% reduction in the annual capacity of CO_2 uptake, though keeping the interannual

404 variability. The annual mean CO_2 uptake in the Bay of Biscay, taking into account the

405 Nightingale's coefficients and wind speed from NCEP/NCAR and QuikSCAT, ranged

406 from -1.3±1.7 (±0.1) $molC \cdot m^{-2} \cdot yr^{-1}$ during 2003 using NCEP/NCAR wind speed and -

407 2.4±2.7 (±0.1) $molC \cdot m^{-2} \cdot yr^{-1}$ during 2004 using QuikSCAT values.

408

409 The empirical relationships developed for each period (see Table 2) were also used to

410 assess the CO_2 exchange in the Bay of Biscay. The disagreements between the *in situ*

411 and modelled CO_2 fluxes are depicted in Figure 5. The mean difference for the entire

412 time series was -0.11±0.51 (±0.02) $molC \cdot m^{-2} \cdot yr^{-1}$ pointing out a slight bias of the

413 estimated algorithms towards fCO_2^{sw} underestimation. The maximum disagreement

414 (~1.81 $molC \cdot m^{-2} \cdot yr^{-1}$) was observed at the beginning of the postbloom 2004 and in

415 general the CO_2 flux was poorly predicted during postbloom periods. The errors

416 reported during the successive years were ~15 and ~21%, respectively, though there are

417 not too significant due to the reduced CO_2 exchange. On the other hand, the best

418 predictions were achieved during prebloom periods, with an error range of 4–6 %.

419

420 DISCUSSION

422   The temporal fCO_2^{sw} distribution during the ECO cruises from November 2002 to

423   December 2004 emphasized the biogeochemical differences at seasonal and interannual

424   scale in the inner part of the Bay of Biscay. An abrupt increase of fCO_2^{sw} values was

425   recorded during winter 2004 but still kept the stronger capacity of CO_2 uptake. So, the

426   longer persistence of winter mixing in 2004 provoked a stronger nutrient fertilization

427   that increased in 1.6 times the NO_3 concentration of the previous year and completely

428   modified the nutrients ratios $NO_3:PO_4$ and $NO_3:Si(OH)_4$ compared to the winter 2003.

430   The different winter mixing conditions each year determined the development and

431   characteristics of the following periods of the seasonal cycle. For example, the fCO_2^{sw} –

432   chl a relationship showed a significant interannual variability during the bloom periods.

433   The intercept of fCO_2^{sw} – chl a for 2003 was close to the *in situ* fCO_2^{atm} levels as

434   expected (Watson et al., 1991; Frankignouille et al., 1996) pointing out the winter air-

435   sea equilibrium once the biological activity is removed. In contrast the intercept of

436   fCO_2^{sw} – chl a relationship for 2004 appreciably exceeded the in situ fCO_2^{atm} level

437   probably associated with intense winter mixing conditions for the 2004 as we explained

438   below. During the 2004 spring bloom, we have observed a strong CO_2 uptake (~289

439   µatm) that does not match with the relatively low surface chl a. We suspect that the

440   lower sampling frequency during 2004 could hinder the observation of chlorophyll

441   maximum.

443   The Eastern North Atlantic Central Waters (ENACW) are formed in the Bay of Biscay

444   by subduction processes during the winter convection when these mode water

445   thermohaline properties are established (Paillet and Mercier, 1997). There is an

446   interannual variation in these properties as the result of variations in the winter air-sea

447   interaction, oceanic heat transport and eddy activity in the formation area.

448   Consequently the prevailing meteorological conditions were analyzed from October to

449   January for both seasonal cycles in order to investigate the reported differences during

450   the formation period of mode waters. Taking into account the water mass distribution in

451   the vicinity of the Bay of Biscay described by Harvey et al. (1982), the latitudinal

452   module of wind was accumulated throughout the winter mixing period. The results

453   (Figure 3) clearly show two different patterns even though wind speed was nearly the

454   same (8 ± 4 m·s^{-1}) for both years. The dominant wind during 2003 was characterized by

455   southern origin (wet and warm) whereas northerly winds (dry and cold) prevailed

456   during the winter mixing of 2004 favouring the longer and deeper winter convection

457   (Pérez et al., 1995). However the nutrient concentrations measured during the ECO

458   cruises even during winter 2004 did not reach the nutrient values previously reported

459   for this region (Treguer et al., 1979; Castro et al., 1998; Pérez et al., 2001). In any case,

460   it seems clear that the meteorological conditions during the formation of the winter

461   mixed layer influence both properties of the mixed layer and their biogeochemical

462   evolution.

463

464   The algorithms performed here to predict fCO_2^{sw} for each period fitted the observed

465   variability with an error lower than 10 µatm. Among measured variables, PO_4 played

466   an outstanding role in the fCO_2^{sw} control during bloom periods explaining 77% of

467   fCO_2^{sw} variability. The photosynthetic absorption and respiration processes were

468   adequately depicted by biological utilisation and rapid remineralization of PO_4 in the

469   surface layer. During postbloom periods, the fCO_2^{sw} distribution was mainly led by

470   temperature. This temperature control of 6.9 µatm·ºC^{-1} disagrees with the isochemical

471 ratio of ~14 $\mu atm \cdot ^\circ C^{-1}$ estimated from the fCO_2^{sw} variability found in the Bay of Biscay

472 (Takahashi et al., 1993). The influence of processes such as mixing waters and

473 phytoplankton uptake altered the theoretical value as previously described by Lüger et

474 al. (2004) in the Eastern North Atlantic Ocean who reported a temperature control of

475 8.7 $\mu atm \cdot ^\circ C^{-1}$. The addition of the nutrient concentration in the assessment of the

476 fCO_2^{sw} algorithm clearly constrains its variability, increasing the fCO_2^{sw} explained

477 variability up to 30%. In fact, compared with previous manuscript where only SST

478 (Stephens et al., 1995; Cosca et al., 2003; Olsen et al., 2004; Feely et al, 2006;

479 Wanninkhof et al., 2006) and chl a (Ono et al., 2004) were considered, we have been

480 able to explain a higher percentage of the fCO_2^{sw} variability with our computed

481 algorithm. Nevertheless, the operational usefulness of the empirical algorithms

482 estimated from nutrients, unlike other computed from SST and chl a, is more limited.

483

484 In spite of this interannual variability, the air-sea fluxes reported similar CO_2 uptake

485 during successive years -1.29±1.68 (±0.09) and -1.7±2.0 (±0.1) $molC \cdot m^{-2} \cdot yr^{-1}$ for 2003

486 and 2004, respectively. From our dataset and using the most frequently used wind

487 speed, we have estimated a CO_2 uptake range from -1.3±1.7 (±0.1) to -2.4±2.7 (±0.1)

488 $molC \cdot m^{-2} \cdot yr^{-1}$ including the value of -1.84 $molC \cdot m^{-2} \cdot yr^{-1}$ for marginal seas between

489 32ºN and 57ºN (Borges et al., 2005). Extrapolating these CO_2 fluxes to the entire Bay

490 of Biscay – limited by the continental slope, 9ºW meridian and 47ºN parallel; $1.9 \cdot 10^{11}$

491 m^2 – the absorbing capacity of atmospheric CO_2 varies between 3 and 5 $TgC \cdot yr^{-1}$.

492 These amounts approximately represent 6% and 10% of the CO_2 drawdown estimated

493 for the North Atlantic Ocean between 45º and 55ºN (Telszewski et al., 2005) in spite of

494 standing for only 5% of its area. The intense CO_2 uptake in the Bay of Biscay compared

495 to average values for the North Atlantic Ocean bears relation to the formation of

496 Eastern North Atlantic Central Water (ENACW). The subduction processes that reach

497 values of 50 -100 m·yr^{-1} (Marshall et al., 1993) isolate CO_2 enriched water during the

498 synthesis and remineralization of organic matter from the surface. Hence the

499 subduction of newly formed ENACW vintages in the Bay of Biscay constitutes a

500 carbon flux to the ocean interior (Marhsall et al., 1993, Follows et al., 1996, Paillet and

501 Mercier, 1997). The oceanic sequestration of atmospheric CO_2 is a decisive process in

502 climatological and geochemical terms (Thiele et al., 1986) therefore its variability,

503 especially in strong sink regions as the Bay of Biscay, should be studied under every

504 climatological conditions.

505

506 CONCLUSIONS

507

508 The underway measurements performed during the ECO cruises using ships of

509 opportunity from November 2002 to December 2004 report an intense CO_2 uptake in

510 the Bay of Biscay. The estimation of CO_2 fluxes ranged from -1.3 to -2.4 molC·m^{-2}·yr^{-1}

511 on a yearly basis, exceeding the sink capacity of the nearby regions of the North

512 Atlantic Ocean.

513

514 The fCO_2^{sw} distribution was correctly predicted from three empirical relationships

515 during prebloom, bloom and postbloom periods reporting errors of ~6.6, ~10 and ~7.7

516 μatm, respectively. Nevertheless the gathered dataset showed differences in the

517 biogeochemical distributions at seasonal and interannual scale. Thus the intense

518 fertilization in winter 2004 was the trigger mechanism for the strong biological uptake

519 during the following spring bloom, supporting the role of the Bay of Biscay as a CO_2

520 sink.

521

Our results highlight the significant effects of physical and biological processes in the uptake capacity of the Bay of Biscay probably steered by meteorological conditions. On the other hand, the use of unattended fCO_2 measuring systems installed on board of ships of opportunity provides valuable information for understanding the CO_2 distribution and the processes affecting its variability at different scales.

527

528

529

530

531

532

533

534

535

536

537

538

539

540

541

542

543

544

545

546

547   REFERENCES

548

549   Andersen, V., Prieur, L., 2000. One-month study in the open NW Mediterranean Sea

550   (DYNAPROC experiment, May 1995): overview of the hydrobiogeochemical strutues

551   an effects of wind events. *Deep-Sea Research I* 47, 397-422.

552

553   Borges, A.V., Delille, B., Frankignoulle, M., 2005. Budgeting sinks and sources of CO_2

554   in the coastal ocean: Diversity of ecosystems counts. *Geophysical Research Letters* 32,

555   L14601, doi:10.1029/2005GL023053.

556

557   Borja, A., Egaña, J., Valencia, V., Franco, J., Castro, R., 2000. 1947-1997, estudio y

558   validación de una serie de datos diarios de temperatura del agua de mar en San

559   Sebastian, procedente de su Aquarium. *Ozeanografika* 3, 139-152.

560

561   Brewer, P.G., Goyet, C., Friederich, G., 1997. Direct observation of the oceanic CO_2

562   increase revisited. *Proceedings of Natural Academic of Science* 94, 8308-8313.

563
564
        Castro, C.G., Pérez, F.F., Holley, S.E., Ríos, A.F., 1998. Chemical characterisation and

565
        modelling of water masses in the Northeast Atlantic. *Progress in Oceanography* 41 (3),

566
        249-279.

567

568   Clayton, T.D., Byrne, R.H., 1993. Spectrophotometric seawater pH measurements: total

569   hydrogen ion concentration scale calibration of m-cresol purple and at-sea results.

570   *Deep-Sea Research II* 40 (10), 2115-2129.

571

572 Cooper, D.J., Watson A.J., Ling, R.D., 1998. Variation of pCO_2 along a North Atlantic

573 shipping route (U.K. to Caribbean): A year of automated observations. *Marine*

574 *Chemistry* 60, 147-164.

575

576 Copin-Montegut, G., Avril, B., 1993. Vertical distribution and temporal variation of

577 dissolved organic carbon in the north-western Mediterranean sea. *Deep-Sea Research II*

578 40 (10), 1963-1972.

579

580 Cosca, C.E., Feely, R.A., Boutin, J., Etcheto, J., McPhaden, M.J., Chavez, F.P.,

581 Strutton, P.G., 2003. Seasonal and interannual CO_2 fluxes for the central and equatorial

582 Pacific Ocean as determined from fCO_2-SST relationships. *Journal of Geophysical*

583 *Research* 108 (C8), 3278, doi:10.1029/2000JC000677.

584

585 DelValls, T.A., Dickson, A.G., 1998. The pH of buffers based on 2-amino-2-

586 hydroxymethil-1,3-propanediol ("tris") in synthetic sea water. *Deep-Sea Research I* 45,

587 1541-1554.

588

589 DOE, 1994. Handbook of methods for the analysis of various parameters of carbon

590 dioxide in seawater; version 2. In: Dickson, A.G., Goyet, C. (Eds.), ORNL/CDIAC-74.

591

592 Dore, J.E., Lukas, R., Sadler, D.W., Kart, D.M., 2003. Climate-driven changes to the

593 atmospheric CO_2 sink in the subtropical North Pacific Ocean. *Nature* 424 (6950), 754-

594 757.

595

596 Feely, R.A., Takahashi, T., Wanninkhof, R., McPhaden, M.J., Cosca, C. E., Sutherland,

597 S.C., 2006. Decadal variability of the air-sea CO_2 fluxes in the equatorial Pacific Ocean.

598 *Journal of Geophysical Research* 111 (C08S90), doi:10.1029/2005JC003129.

599

600 Follows, M.J., Williams, R.G., Marshall, J.C., 1996. The solubility pump of carbon in

601 the subtropical gyre of the North Atlantic. *Journal of Marine Research* 54, 605-630.

602

603 Frankignoulle, M., Bourge, I., Canon, C., Dauby, P., 1996. Distribution of surface

604 seawater partial CO_2 pressure in the English Channel and in teh Southern Bight of the

605 North Sea. *Continental Shelf Research* 16, 381-395.

606
607
Gonzalez-Davila, M., Santana-Casiano, J.M., Rueda, M.J., Llinas, O., Gonzalez-Davila,
608
E.F., 2003. Seasonal and interannual variability of sea-surface carbon dioxide species at
609
the European Station for Time Series in the Ocean at the Canary Islands (ESTOC)
610
between 1996 and 2000. *Global Biogeochemical Cycles* 17 (3), 1076.

611

612 Goyet, C., Millero, F., O'Sullivan, D.W., Eischeid, G., McCue, S.J., Bellerby, R.G.J.,

613 1998. Temporal variation of pCO_2 in surface seawater of the Arabian Sea in 1995.

614 *Deep-Sea Research II* 45, 609-623.

615

616 Gruber, N., Sarmiento, J.L., Stocker, T.F., 1996. An improved method for detecting

617 anthropogenic CO_2 in the oceans. *Global Biogeochemical Cycles* 10 (4), 809-837.

618

619 Gruber, N., 1998. Anthropogenic CO_2 in the Atlantic Ocean. *Global Biogeochemical*

620 *Cycles* 12, 165-191.

621

622 Gruber, N., Keeling, C.D., Bates, N.R., 2002. Interranual variability in the North

623 Atlantic Ocean carbon sink. *Science* 298, 2374-2378.

624

625 Hansen, H.P., Grasshoff, K., 1983. Automated chemical analysis. In. K. Grasshoff, M.

626 Ehrhardt and K. Kremling (eds.). Methods of Seawater Analysis. 2nd ed. Verlag

627 Chemie, Weinheim. pp. 368-376.

628

629 Harvey, J., 1982. θ-S relationships and water masses in the eastern North Atlantic.

630 *Deep-Sea Research II* 29 (8A), 1021-1033.

631

632 Haynes, R., Barton, E.D., 1991. Langranian observations in the Iberian coastal

633 transition zone. *Journal of Geophysical Research* 96 (C8), 14731-14741.

634

635 Ho, D.T., Law, C.S., Smith, M.J., Schlosser, P., Harvey, M., Hill, P., 2006.

636 Measurements of air-sea gas exchange at high wind speeds in the Southern Ocean:

637 Implications for global parameterizations. *Geophysical Research Letters* 33, L16611,

638 doi:10.1029/2006GL026817.

639

640 Hood, E.M., Merlivat, L., Johannessen, T., 1999. Variations of fCO$_2$ and air-sea flux of

641 CO$_2$ in the Greenland sea gyre using high-frequency time series data from CARIOCA

642 drift buoys. *Journal of Geophysical Research* 104 (C9), 20571-20583.

643

644 Hood, E.M., Merlivat, L., 2000. Annual to interannual variations of fCO_2 in the

645 northwestern Mediterranean Sea: Results from hourly measurements made by

646 CARIOCA buoys, 1995-1997. Journal of Marine Research 59, 113-131.

647

648 Kalnay, E., Kanamitsu, M., Kistler, R., Collins, W., Deaven, D., Gandin, L., Iredell, M.,

649 Saha, S., White, G., Woollen, J., Zhu, Y., Chelliah, M., Ebisuzaki, W., Higgins, W.,

650 Janowlak, J., Mo, K.C., Ropelewski, C., Wang, J., Leetmaa, A., Reynolds, R., Jenne, R.,

651 Joseph, D., 1996. The NCEP/NCAR Reanalysis Project. Bulletin American

652 Meteorological Society 77, 437-471.

653

654 Kara, A.B., Rochford, P.A., Hurlburt, H.E., 2000. An optimal definition for ocean

655 mixed layer depth. Journal of Geophysical Research 105 (7), 16803-16821.

656

657 Körtzinger, A., Kowve, W., Kähler, P., Mintrop, L., 2001. C:N ratios in the mixed layer

658 during productive season in the northeast Atlantic Ocean. Deep-Sea Research I 48, 661-

659 688.

660

661 Le Quere, C., Orr, J.C., Monfray, P., Aumont, O., Madec, G., 2000. Interannual

662 variability of the oceanic sink of CO2 from 1979 through 1997. Global Biogeochemical

663 Cycles 14 (4), 1247-1265.

664

665 Lee, K., Wanninkhof, R., Takahashi, T., Doney, S.C., Feely, R.A. 1998. Low

666 interannual variability in recent oceanic uptake of atmospheric carbon dioxide. *Nature*

667 396, 155-159.

668

669 Lefévre, N., Taylor, A., 2002. Estimating pCO_2 from sea surface temperatures in the

670 Atlantic Gyres. *Deep-Sea Research I* 49, 539-554.

671

672 Lévy, M., Mémery, L., André, J.-M., 1998. Simulation of primary production and

673 export fluxes in the Northwestern Mediterranean Sea. *Journal Marine Research* 56,

674 197-238.

675

676 Lochte, K., Ducklow, H.W., Fasham, M.J.R., Stienen, C., 1993. Plankton succession

677 and carbon cycling at 47ºN 20ºW during the JGOFS North Atlantic Bloom Experiment.

678 *Deep-Sea Research I* 40 (1/2), 91-114.

679

680 Lueker, T.J., Dickson, A.G., Keeling, C.D., 2000. Ocean pCO_2 calculated from

681 dissolved inorganic carbon, alkalinity, and equations for K1 and K2 : validation based

682 on laboratory measurements of CO_2 in gas and seawater at equilibrium. *Marine*

683 *Chemistry* 70, 105-119.

684
685 Luger, H., Wallace, D.W.R., Kortzinger, A., Nojiri, Y., 2004. The pCO_2 variability in

686 the midlatitude North Atlantic Ocean during a full annual cycle. *Global*

687 *Biogeochemical Cycles* 18 (3), GB3023, doi:10.1029/2003GB002200, 2004.

688

689 Maier-Reimer, E., Hasselmann, K., 1987. Tansport and storage of CO_2 in the ocean - an

690 inorganic ocean-circulation carbon cycle model. *Climate Dynamics* 2, 63-90.

691

692 Marshall, J.C., Nurser, A.J.G., Williams, R.G., 1993. Inferring the subduction rate and

693 period over North Atlantic. *Journal of Physical Oceanography* 23, 1315-1329.

694

Metzl, N., Poisson, A., Louanchi, F., Brunet, C., Schauer, B., Bres, B., 1995. Spatio-temporal distributions of air-sea fluxes of CO_2 in the Indian and Antarctic Oceans. *Tellus* 47B, 56-69.

Mouriño, C., Fraga, F., 1985. Determinación de nitratos en agua de mar. *Investigación Pesquera* 49, 81-96.

Nelson, N.B., Bates, N.R., Siegel, D.A., Michaels, A.F., 2001. Spatial variability of the CO_2 sink in the Sargasso Sea. *Deep-Sea Research II* 48, 1801-1821.

Nightingale, P.D., Malin, G., Law, C.S., Watson, A.J., Liss, P.S., Liddicoat, M.I., Boutin, J., Upstill-Goddard, R.C., 2000. In situ evaluation of air-sea exchange parameterizations using novel conservative and volatile tracer. *Global Biogeochemical Cycles*, 14, 373-387.

Olsen, A., Bellerby, R.G.J., Johannessen, J., Omar, A.M., Skjelvan, I., 2003. Interannual variaiblity in the wintertime air-sea flux of carbon dioxide in the norhtern Norht Atlantic. *Deep-Sea Research I* 50, 1323-1338.

Olsen, A., Triñanes, J.A., Wanninkhof, R., 2004. Sea–air flux of CO_2 in the Caribbean Sea estimated using in situ and remote sensing data. *Remote Sensing of Environment* 89 (3), 309-325.

717

718
719
720
721
Olsen A., Wanninkhof R., Trinanes J.A., Johannessen T., 2005. The effect of wind speed products and wind speed-gas exchange relationships on interannual variability of the air-sea CO_2 gas transfer velocity. *Tellus B* 57 (2), 95-106.

722
723
724
725
Olsen, A., Triñanes, J., Wanninkhof, R., 2004. Sea-air flux of CO_2 in the Caribbean Sea estimated using *in situ* and remote sensing data. *Remote Sensing of Environment* 89, 309-325.

726
727
728
729
Ono, T., Saino, T., Kurita, N., Sasaki, K., 2004. Basin-scale extrapolation of shipboard pCO_2 data by using satellite SST and Chla. *International Journal of Remote Sensing* 25 (19), 3803-3815.

730
731
732
733
Padin, X.A., Vázquez-Rodríguez, M., Ríos, A.F., Pérez, F.F., 2007a. Atmospheric CO_2 measurements and error analysis on seasonal air-sea CO_2 fluxes in the Bay of Biscay. *Journal of Marine Systems*, doi:10.1016/j.jmarsys.2006.05.010.

734
735
736
737
Padin, X.A., Vázquez-Rodríguez, M., Ríos, A.F., Pérez, F.F., 2007b. Surface CO_2 measurements in the English Channel and Southern Bight of North Sea using voluntary observing ships. *Journal of Marine Systems*, doi:10.1016/j.jmarsys.2006.05.011.

738
739
740
Paillet, J., Mercier, H., 1997. An inverse model of the eastern North Atlantic general circulation and thermocline ventilation. *Deep-Sea Research II* 44 (8), 1293-1328.

741
742
Pérez, F.F., Fraga, F., 1987. A precise and rapid analytical procedure for alkalinity determination. *Marine Chemistry* 21, 169-182.

743

744 Pérez, F.F., Ríos, A.F., King, B.A., Pollard, R.T., 1995. Decadal changes of the θ-S

745 relatioship of the Eastern North Atlantic Central Water. *Deep-Sea Research II* 42

746 (11/12), 1849-1864.

747

748 Pérez, F.F., Castro, C.G., Álvarez-Salgado, X.A., Ríos, A.F., 2001. Coupling between

749 the Iberian basin-scale circulation and the Portugal boundary current system: a

750 chemical study. *Deep-Sea Research I* 48, 1519-1533.

751

752 Pérez, F.F., Alvarez, M., Ríos, A.F., 2002. Improvements on the back-calculation

753 technique for estimating anthropogenic CO_2. *Deep-Sea Research I* 49 (5), 859-875.

754

755 Peylin, P., Rayner, P.J., Bousquet, P., Carouge, C., Hourdin, F., Heinrich, P., Ciais, P.,

756 2005. Daily CO_2 flux estimates over Europe from continuous atmospheric

757 measurements: 1, inverse methodology. *Atmospheric Chemistry and Physics* 5, 3173-

758 3186.

759

760 Sabine, C.L., Feely, R.A., Gruber, N., Key, R.M., Lee, K., Bullister, J.L., Wanninkhof,

761 R., Wong, C.S., Wallace, D.W.R., Tilbrook, B., Millero, F.J., Peng, T.H., Kozyr, A.,

762 Ono, T., Rios, A.F., 2004. The oceanic sink for anthropogenic CO_2. *Science* 305

763 (5682), 367-371.

764

765 Sarmiento, J.L., 1995. Modeling the oceanic uptake of anthropogenic carbon. U.S.

766 JGOFS News: 4-6.

767

768 Sarmiento, J.L., Sundquist, E.T., 1992. Revised budget for the oceanic uptake of

769 anthropogenic carbon dioxide. *Nature* 356, 589-593.

770

771 Stephens, M.P., Samuels, G., Olson, D.B., Fine, R.A., Takahashi, T., 1995. Sea-air flux

772 of CO_2 in the north Pacific using shipboard and satellite data. *Journal of Geophysical*

773 *Research* 100 (C7), 13571-13583.

774

775 Sweeney, C., Gloor, E.M., Jacobson, A.R., Key, R.M., Galen, M., Sarmiento, J.F. and

776 Wanninkhof, R. 2007. Constraining Global air-sea Gas Exchange for CO_2 with recent

777 Bomb ^{14}C measurements. *Global Biogeochemical Cycles* 21 (2), GB2015,

778 doi:10.1029/2006GB002784.

779

780 Takahashi, T., Feely, R.A., Weiss, R.F., Wanninkhof, R.H., Chipman, D.W., 1997.

781 Global air-sea flux of CO_2: An estimate based on measurements of sea-air pCO_2

782 difference. *Proceedings of Natural Academic of Science* 94, 8292-8299.

783

784 Takahashi, T., Olafsson, J., Goddard, J.G., Chipman, D.W., Sutherland, S.C., 1993.

785 Seasonal variation of CO_2 and nutrients in the high-latitude surface oceans: a

786 comparative study. *Global Biogeochemical Cycles* 7 (4), 843-878.

787

788 Takahashi, T., Sutherland, S.C., Sweeney, C., Poisson, A., Metzl, N., Tilbrook, B.,

789 Bates, N., Wanninkhof, R., Feely, R.A., Sabine, C., Olafsson, J., Nojiri, Y., 2002.

790 Global Sea-Air CO_2 flux based on climatological surface ocena pCO_2 and seasonal

791 biological and temperature effects. *Deep-Sea Research II* 49, 1601-1622.

792

793   Tans, P. P., Fung, I. Y., Takahashi, T., 1990. Observational Constraints on the global

794   atmospheric CO_2 budget. *Science* 247, 1431-1438.

795

796   Telszewski, M., Schuster, U., Watson, A.J., Olsen, A., Johannessen, T., Gonzalez-

797   Davila, M., Steinhoff, T., Wallace, D.W.R., Körtzinger, A., 2006. Variability of the

798   CO_2 air-sea exchange on a seasonal scale in the North Atlantic derived from shipboard

799   measurements in 2005. IP CARBOOCEAN report (deliverables D4.3 and D4.4).

800
801
    Treguer, P., Le Corre., P., Grall, J.R., 1979. Seasonal variations of nutrients in the

802   upper waters of the Bay of Biscay and their relation to phytoplankton growth. *Deep-Sea*

803   *Research I* 26 (10), 1121-1152.

804

805   Unesco, 1986. Progress on oceanographic tables and standards 1983-1986. Work and

806   recomendations of UNESCO/SCOR/ICES/IAPSO Joint panel. UNESCO Technical

807   Papers in Marine Science 50.

808

809   Wallace, D.W.R., 1995. Monitoring global ocean carbon inventories. Ocean Observing

810   System Development Panel, OOSDP Background Report No. 5, Texas A&M

811   University, College Station, TX, 54pp.

812

813   Wanninkhof, R., Olsen, A., Trinanes, J., 2007. Air-sea CO_2 fluxes in the Caribbean Sea

814   from 2002-2004. *Journal of Marine Systems* 66 (1), 272-284.

815

816   Watson, A.J., Robinson, C., Robinson, J.E., Williams, P.J. le B., Fasham, M.J.R., 1991.

817   Spatial variability in the sink for atmospheric carbon dioxide in the North Atlantic.

818   *Nature* 350, 50-53.

819

820   Weiss, R.F., 1974. Carbon dioxide in water and seawater: the solubility of non-ideal

821   gas. *Marine Chemistry* 2, 203-215.

822

823   Yentsch., C.S., Menzel, D.W., 1963. A method for the determination of phytoplankton

824   chlorophyll and phaeophytin by fluorescence. *Deep-Sea Research* 10 (3), 221-231.

825

826

827

828

829

830

831

832

833

834

835

836

837

838

839

840

841   FIGURE CAPTIONS

842

843   Figure 1: Map of the study area showing the regular route (black line) and the four

844   sampling stations (white circles) in the inner part of the Bay of Biscay.

845

846   Figure 2: Mean values of the four stations during each cruise of sea surface temperature

847   (SST; white circles), sea surface salinity (SSS; grey circles), phosphate (PO_4; white

848   circles), silicate ($Si(OH)_4$; grey circles) and nitrate concentration (NO_3; dark grey

849   circles), chlorophyll *a* concentration (chl a; white circles), oxygen (O_2; grey circles) and

850   CO_2 fugacity in the seawater (black circles) and the atmosphere (dotted line).

851

852   Figure 3: Mixed layer depth throughout the following 215 days from 1st October of the

853   winter mixing period of 2003 (black line) and 2004 (grey line) estimated from

854   MERCATOR-OCEAN model. Accumulated latitudinal component of wind speed

855   during the same period retrieved from QuikSCAT sensor at averaged point (45ºN 6ºW)

856   during 2003 (white circle) and 2004 (grey circle).

857

858   Figure 4: a) Average values of the four stations of chlorophyll *a* concentration (white

859   circles) and the monthly distribution of fCO_2^{sw} at the mean sea surface temperature at

860   annual scale ($^BfCO_2^{sw}$, black circles) and the annual mean fCO_2^{sw} value corrected for

861   changes in temperature ($^TfCO_2^{sw}$, grey circles). b) Average values of observed fCO_2^{sw}

862   (white circles) for each ECO transect in the Bay of Biscay and monthly variation of

863     $^BfCO_2^{sw}$ meaning biological control (black bar) and $^TfCO_2^{sw}$ meaning temperature

864   control (grey bar).

865

866 Figure 5: Interpolated values from weekly averages of air-sea CO_2 flux estimated in the

867 Bay of Biscay (thick line) and of flux anomalies associated to fCO_2^{sw} estimation using

868 empirical relationships (fine line) as well as mean values for each period and for the

869 entire sampled period. Interpolated values of wind speed obtained from QuikSCAT

870 sensor (grey thick line) and NCEP/NCAR reanalysis model (grey fine line).

871

872

873

874

875

876

877
878
879
880
881
882
883
884
885
886
887
888
889
890
891
892
893
894
895
896
897
898
899
900
901
902
903
904
905
906
907
908
909
910

911
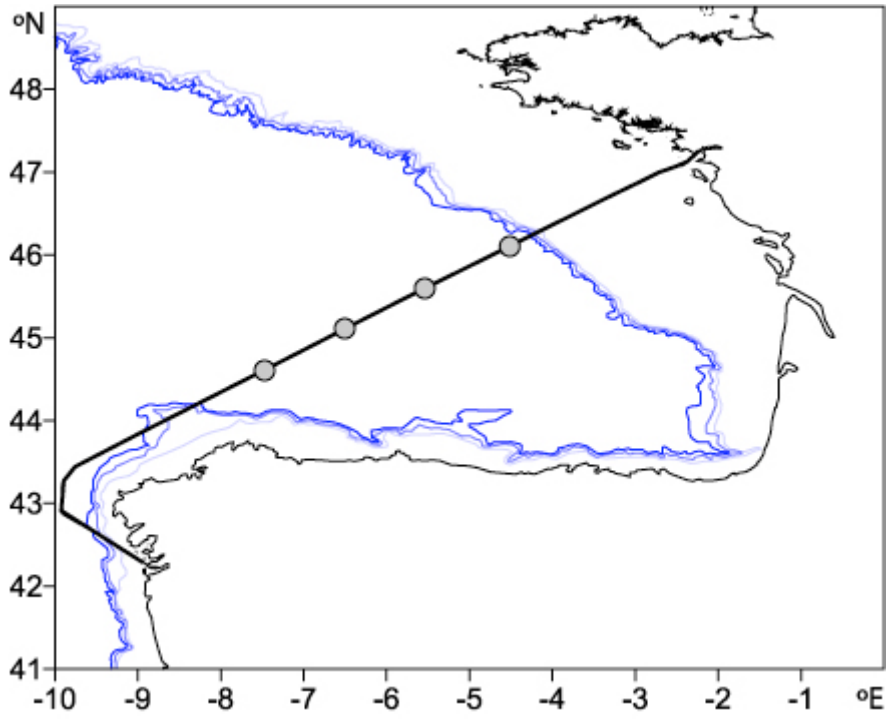
912

913

914   Figure 1

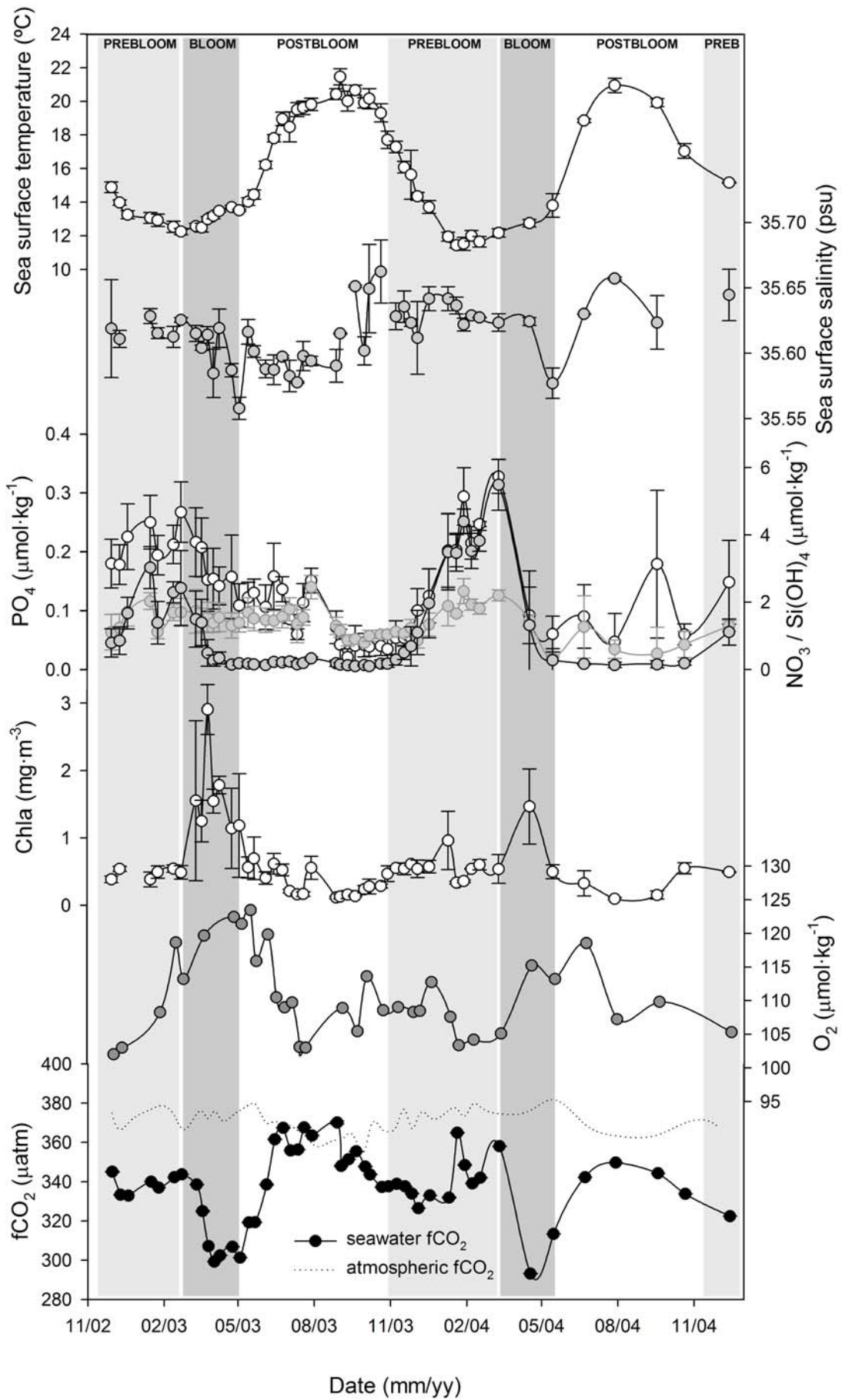915

916

917

918

919

920

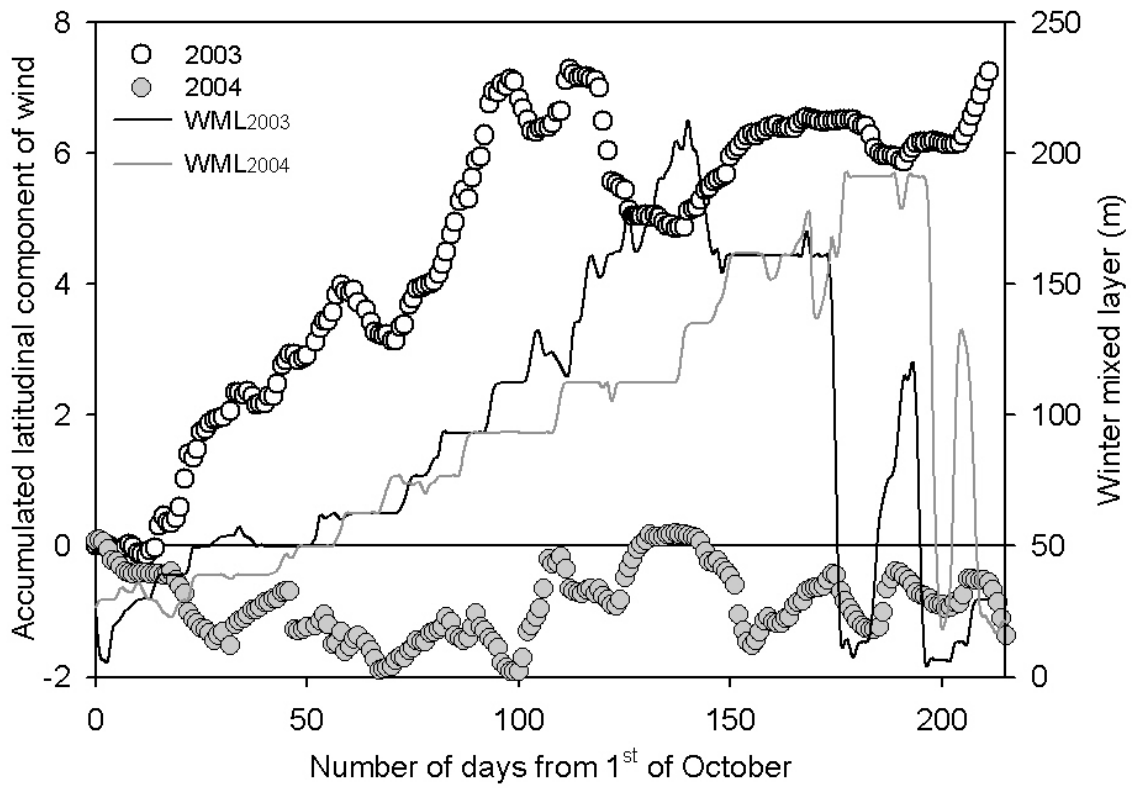921

922

923

924

926   Figure 2

927

928

929   Figure 3

930

931

932

933

934
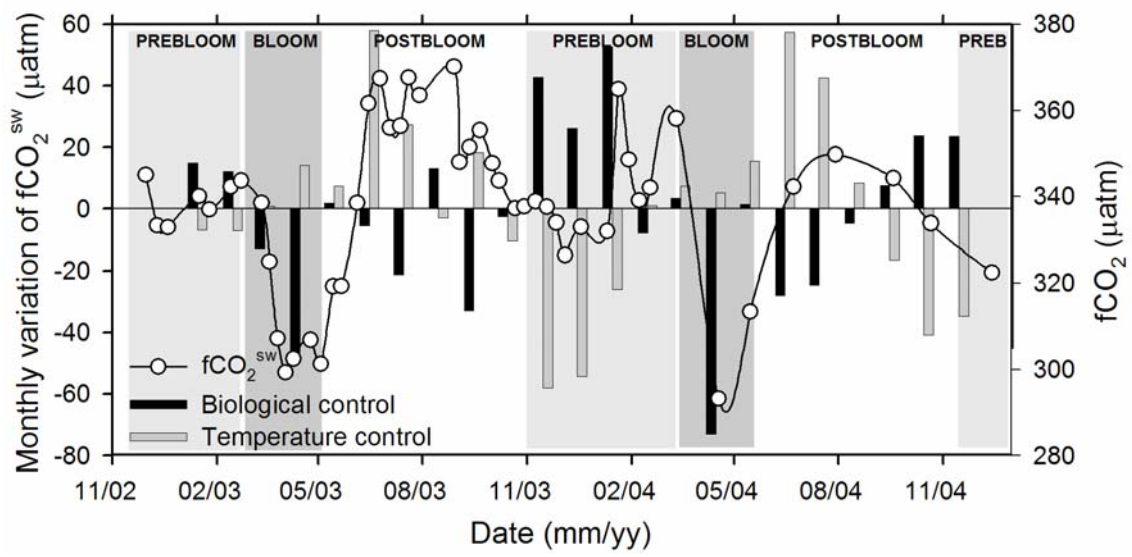
935

936

937

938

939

940

941

942

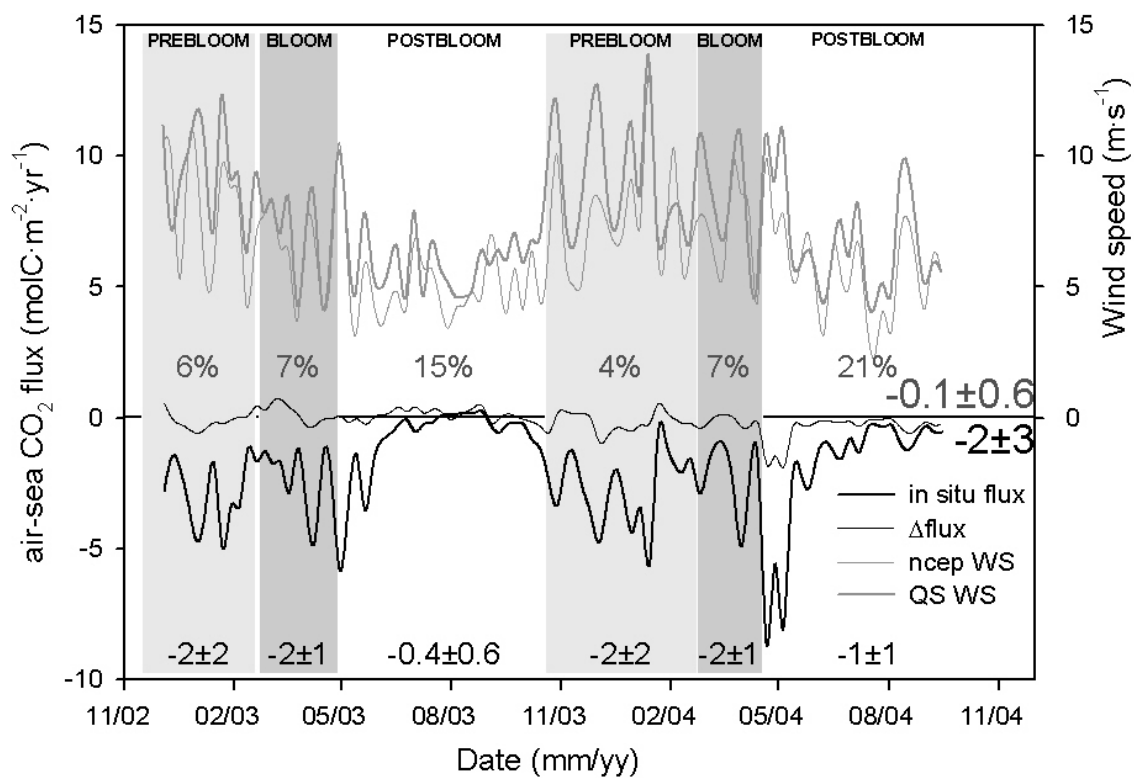943 Figure 4

944

945

946

947

948

949

950

951

952   Figure 5

953

954

955

956

957

958

959

960

961

962

963

964
965